

# Analysis of Ground Movements in Shield Tunneling and Their Effects on Adjacent Bridge Pile Foundations

Yongyue Hu<sup>1,2</sup>, Changhong Li<sup>1,2,\*</sup> and Juzhou Li<sup>1,2</sup>

<sup>1</sup> School of Civil and Resource Engineering, University of Science and Technology Beijing, Beijing 100083, China

<sup>2</sup> Beijing Key Laboratory of Urban Underground Space Engineering, University of Science and Technology Beijing, Beijing 100083, China

Received 01 September 2023; Accepted 12 November 2023

## Abstract

The movement of the ground and the redistribution of stress caused by shield tunneling result in deformations and changes in internal forces in bridge pile foundations, which, in turn, affect the safety of pile superstructure. A numerical computational model based on the modified Mohr–Coulomb (MMC) criterion was proposed to analyze the effects of shield tunneling on the stability of the pile foundations of existing bridges during the early, middle, and late stages of shield tunnel construction. A 3D numerical model of the shield tunnel and bridge pile foundation was constructed using the finite element software Midas GTSNX. The ground movements and deformation patterns of pile foundations were analyzed throughout the entire shield tunneling process beneath existing bridge pile foundations. Results demonstrate that utilizing the elastic-plastic constitutive model founded on the MMC criterion is more effective for illustrating the surface settlement pattern induced by shield tunnel construction. Bridge piles are continuously deforming during the construction of a shield tunnel. The deformation of a bridge pile is maximized when a shield tunnel reaches the foundation of the pile. The deformation of bridge pile foundations remains stable after passage. The deformation and bending moments of bridge pile foundations decrease with an increase in distance from the tunnel. The influence on bridge pile foundations is reduced with an increase in distance from the shield tunnel. This study provides a good reference for the construction quality control and safety assessment of similar tunnel projects.

*Keywords:* Shield tunnel, Existing bridge piling, MMC criterion, Numerical analysis

## 1. Introduction

Ground-level rail transit lines, elevated overpasses, and other necessary road facilities are constantly being improved to accompany the continuous development of Chinese cities [1]. Moreover, the scale of underground space development and utilization has expanded. The shield method [2] is widely employed in underground road projects worldwide because of its high mechanization level; low environmental effect; lack of restriction by factors such as topography and geomorphology; and significant safety, efficiency, and economy. More than 90% of tunnels in developed countries are constructed using the shield method, and China has become a major player in the tunneling industry with a global market share of approximately 60% [3].

However, technical challenges associated with tunnel construction continue to escalate, because factors, such as existing building foundations, regional engineering geology, and hydrogeological conditions, should be considered in new tunnel construction. Tunneling thrust [4-7], grouting pressure [8-11], and excavation disturbance generated by shield tunneling can result in the stress concentration and deformation of the surrounding building pile foundations, and the subsidence of the surrounding ground [12]. Furthermore, the stability of the foundations of surrounding buildings has been increasingly affected by the growing size of the shield machine and the construction of a shield tunnel.

Although researchers [13-15] have extensively studied the effects of shield tunnel construction on the stability of

adjacent buildings and ground settlement through theoretical and numerical simulations. However, research remains insufficient on the constitutive model and parameter values of geotechnical soil in the simulation and analysis of shield tunneling, along with the deformation mechanism of the pile foundation throughout the entire cycle of shield tunnel construction.

To analyze the ground movements and effects on adjacent bridge pile foundations caused by a shield tunnel crossing the bridge pile foundations during the early, middle, and late stages of boring, the geological investigation data, soil body ontology model, and spatial relationship between the pile foundations of Shenzhen Bay Bridge and the tunnel based on the rapid transformation project of Wanghai Road in Shenzhen were fully considered. This study provides a good reference for the construction quality control and safety assessment of similar tunnel projects.

## 2. State of the art

Extensive research has been conducted by scholars on the effects of shield tunnel construction on neighboring structures. On the basis of the genetic algorithm (GA) and the bidirectional long short-term memory network (Bi-LSTM) structure, the GA–Bi-LSTM prediction model for the settlement of existing tunnels was constructed by Zhou et al. [16]. This model considered engineering geological, spatial, and shield construction parameters. However, engineering geological parameters are variables that change

\*E-mail address: hyy\_ustb19@126.com

ISSN: 1791-2377 © 2023 School of Science, THU. All rights reserved.

doi:10.25103/jestr.166.05

during the construction stage and not considered by the model. To address the issue of appropriate grouting volume and pressure in shield tunnel construction, Wang et al. [17] conducted a study by using a two-factor multistage orthogonal test; however, the deformation law under the interaction between the pile–soil interface was not reflected by the Mohr–Coulomb (MC) criterion employed in the computational model. The effect of grouting pressure fluctuation on the deformation of adjacent pile foundations during shield construction was investigated by Zhang et al. [18] through numerical simulation. However, the deformation pattern of pile foundations during the entire shield construction process was not analyzed. Zhou et al. [19] and Huang et al. [20] conducted dynamic analysis of surface settlement and pile deformation by using Midas GTSNX finite element software throughout the entire shield excavation process. They determined the pile deformation law before and after the shield tunnel passed through the pile foundation of a bridge. However, the influence of the constitutive model of the material on the calculation results was not adequately considered. To quantify the effect of shield excavation on surface settlement, Yang et al. [21] proposed the use of centrifuge tests to simulate the dynamic process of constructing an oversized diameter shield tunnel near a railroad. However, the mechanical properties of the test materials were not evaluated. With regard to the surface uplift and tube sheet uplift caused by underwater tunnel construction, Gao et al. [22] used a combination of finite element software analysis and measured data to investigate surface deformation patterns throughout the entire process of constructing a double-lane shield tunnel under a river. However, research on stratigraphic constitutive models is still lacking.

To investigate the change in soil stiffness during tunnel excavation, Soomro et al. [23] studied the response of pile foundations to subsequent tunnel construction after the initial tunnel excavation in the case of double-tunnel excavation. However, further exploration into the deformation patterns of pile foundations throughout the entire tunnel construction process is still insufficient. On the basis of an advanced 3D elastic-plastic coupled consolidation analysis method, Lee et al. [24] investigated the effects of overrun cut-and-cover tunnels on the bending moments and axial structural load distribution of loaded piles. However, the selection of principal and material parameter values was not studied exhaustively. The effect of building stiffness on pile settlement was investigated by Simic-Silva et al. [25] through the numerical simulation of excavation on both sides of a tunnel located within a London clay layer. However, the effect of soil shear hardening on ground settlement was not considered. In terms of the influence of shield construction on surface settlement, Repetto et al. [26] innovatively applied a procedure to optimize the management of the construction phase. This procedure was verified by combining theoretical analysis and numerical simulation results. However, the effect of the entire process of shield tunnel construction on surface settlement was not analyzed. To understand the influences of dynamic processes, such as shield tunnel excavation, staged construction, and tube lining installation, on surface settlement, Allahverdi et al. [27] developed a detailed numerical model for analysis. However, they did not conduct a thorough analysis of the model's principles and parameter values, nor did they analyze the overall influence of shield tunnel construction on surface settlement. The problem of ground settlement caused by shield tunnel

excavation was studied using the tunnel excavation equipment developed by Lee et al. [28]. However, the dynamic process of tunnel excavation was not sufficiently analyzed. The problem of limitations in existing pressure transfer theories during shield tunnel excavation was effectively solved by Zizka et al. [29-30]. They introduced a new method for accurately describing pressure transfer in the support. However, the variation in the shear modulus of soil during construction progress was not considered. In terms of constitutive modeling, Lavasan et al. [31] utilized an elastic-plastic constitutive model with a double hardening rule to examine the effects of mud-water shield tunnel excavation on ground settlement and lining forces in fully saturated soil with varying hydraulic conductivities. However, the effect of the shield tunnel construction phase on ground settlement was not addressed. Filho [32] and Bilgin [33] analyzed the influence of shield tunnel construction on the deformation of surface buildings across different strata by using engineering examples. However, a research gap that specifically focuses on the soil constitutive model and the deformation characteristics of the soil body through which the tunnel passes exists. The effects of the mechanical properties of rocks and soil on shield tunneling were extensively examined by Erharter [34] and Bach [35]. However, a comprehensive dynamic analysis of the entire tunneling process was not conducted.

Construction parameters and modeling tests are currently the focus of most studies, which aim to assess the effect of shield tunnels on building pile foundations. However, research is limited on the evolution of pile foundation deformation in relation to the constitutive models of rock and soil, and its relation to the entire process of shield tunnel construction passing through buildings. In the current study, a 3D finite element model was constructed using Midas GTSNX finite element software, and the principles of selecting the values for the relevant parameters of the modified MC (MMC) criterion were proposed. The settlement, lateral movement, and ground deformation patterns of bridge foundation piles induced by shield tunnels crossing bridge foundations were analyzed at the initial, intermediate, and final stages of shield tunneling through bridge foundations. The results can serve as a reference for predicting the effects of construction on strata and buildings in future tunneling projects on the site. In addition, the study made recommendations for reducing potential disturbances to neighboring buildings during shield construction.

The remainder of this study is organized as follows. Section 3 outlines the spatial relationship between bridge pile foundations and a shield tunnel. It also describes the MMC criterion and the employed parameter estimation method. Moreover, a 3D numerical calculation model of the shield tunnel is constructed. Section 4 investigates the deformation and stress evolution of the entire bridge pile foundations during the early, middle, and late stages of tunnel construction. Section 5 summarizes the conclusions.

### 3. Methodology

#### 3.1 Physical model

The Wanghai Road Expressway improvement project is located in Nanshan District, Shenzhen City, China. It encompasses two components: the construction of the new underground expressway and the renovation of the main road above the ground. In accordance with the current site conditions, the construction program for the underground

section was divided into two sections: the shield construction and open cut construction sections. The maximum depth of the structural base plate of the shield section was about 46.5 m, ground elevation was

approximately 3.06-5.22 m, the outer diameter was 16.28 m, and the inner diameter was 15.7 m. The positional relationship between the shield tunnel and Shenzhen Bay Bridge is depicted in Fig. 1.

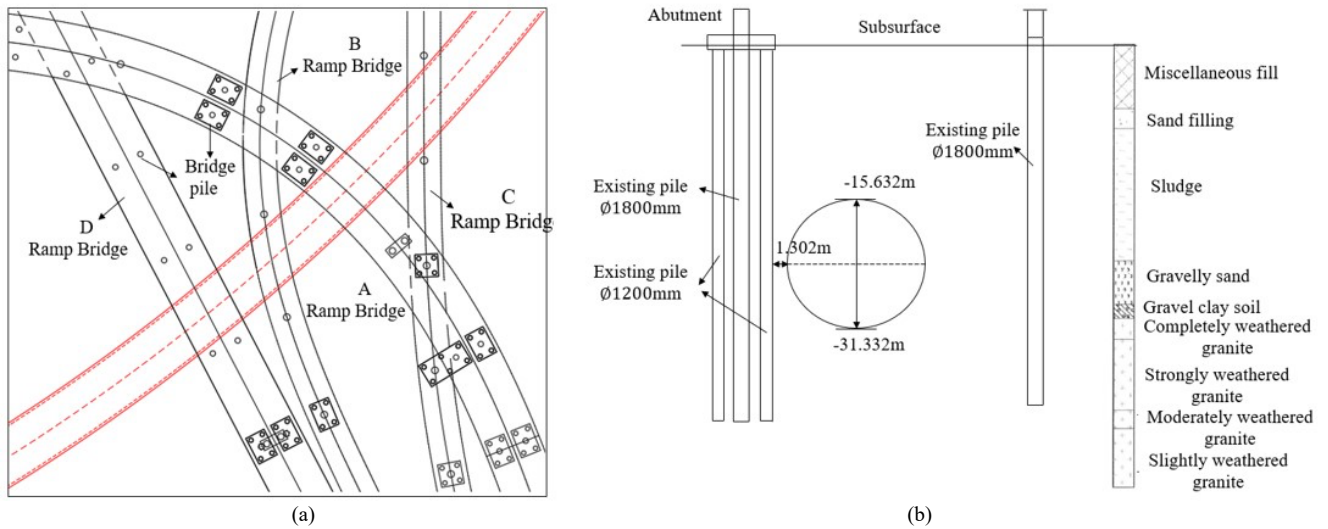


Fig. 1. Relationship between Wanghai Road tunnel and bridge and pile foundation.

Note: (a) Relationship between the tunnel and the bridge on Wanghai Road. (b) Diagram of Ramp A bridge piles in relation to the tunnel

Shenzhen Bay Bridge connects Shenzhen and Hong Kong, with four ramp bridges, i.e., A, B, C, and D, on the Shenzhen side. The pile foundation of the bridge consists of two parts: pier and pile body. Pier diameter is 1.5 m, while pile diameter is 1.8 m. The pile end enters into the medium weathered rock holding layer, and the design is an end-bearing pile. Wanghai Road Tunnel plane centerline, side through Shenzhen Bay Bridge Ramp Bridges A, B, C, and D, for a total of 11 bridge piles.

In accordance with the detailed geological investigation report, the project area falls within the exploration range of the stratum and geotechnical parameters, as indicated in Table 1. The shield section is southeast, adjacent to Shenzhen Bay Park sea. The distance is about 40 m. The water surface exhibits tidal changes. The ground stabilizes a water level depth of 1.60-6.40 m. The stabilization of water level elevation is from -2.91 m to 3.62 m.

Table 1. Parameters related to geotechnical materials.

Geological layer	Compression Modulus $E_s/MPa$	Poisson's ratio $\mu$	Unit weight $\gamma/kN \cdot m^{-3}$	Internal friction angle $\varphi/^\circ$	Cohesive force $C/kPa$
Miscellaneous fill	4.56	0.35	18.5	16.2	28.40
Sand filling	2.36	0.42	16.5	1.00	16.15
Sludge	5.50	0.30	19.5	3.90	20.80
Gravelly sand	4.19	0.25	20.0	31.3	19.57
Completely weathered	4.29	0.30	19.5	23.3	24.37
Strongly weathered	1500	0.25	25.1	29.8	1800
Moderately weathered	7280	0.22	27.0	42.0	3400
Slightly weathered	97000	0.20	29.0	41.8	3330

Note: Fully weathered, strongly weathered, moderately weathered, and slightly weathered represent various degrees of granite weathering.

### 3.2 Numerical models

On the basis of the spatial relationship between Wanghai Road Underground Expressway and Shenzhen Bay Bridge in Section 3.1, and the geological investigation data, Midas finite element software was utilized to create a 3D solid model for the excavation of the shield tunnel. The geometric model's boundary should be greater than 3-4 times the depth of the tunnel base. Moreover, the vertical depth of the whole model should be larger than 2-4 times the depth of the tunnel base. Therefore, the model was established with dimensions of 108 m×182 m×81 m in the X, Y, and Z directions (Fig. 2).

In Fig. 2, A-A, B-B, and C-C represent the three profiles of the vertical shield tunnel alignment. In addition, A1, B1, C1, and D1 correspond to the bridge piles of the four ramp bridges that are nearest to the shield tunnel.

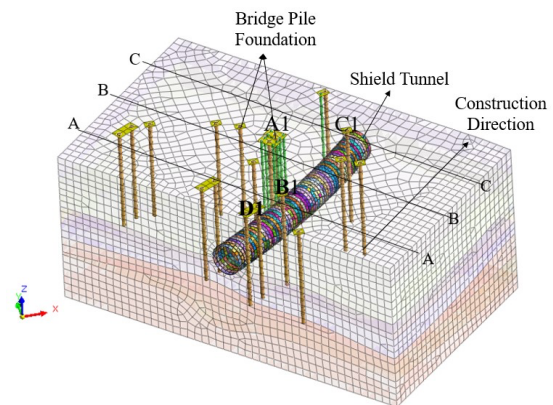


Fig. 2. Shield Excavation Calculation Model

**3.3 MMC criterion**

The MC criterion is commonly employed in general geotechnical engineering. However, it assumes that the studied object is an ideal elastic-plastic body, which better describes the damage behavior of soil, but it does not account for the effect of stress history or the resilient modulus of soil during elastic unloading or loading. To resolve the instability issue of the MC criterion in the plastic strain direction at the vertex of the off-plane hexagonal calculation, the MMC criterion introduces off-plane rounding, resulting in the enhanced convergence of model calculation and augmented numerical model calculation reliability, as illustrated in Fig. 3.

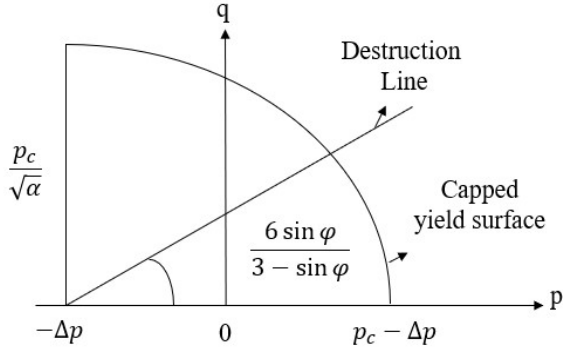


Fig. 3. MMC criterion structure in the p-q plane yielding criterion

The MMC criterion is a dual-hardening model that features independent yield surfaces for both shear and compression. It can be expressed in the partial plane as the MC equation in terms of  $R_1(\theta)$  and  $R_2(\theta)$ :

$$f_1 = \frac{q}{R_1(\theta)} - \frac{6 \sin \varphi}{3 - \sin \varphi} (p + \Delta p) = 0 \tag{1}$$

$$f_2 = (p + \Delta p)^2 + \alpha \left[ \frac{q}{R_2(\theta)} \right]^2 - p_c^2 = 0 \tag{2}$$

In the formula,  $R_1(\theta) = \left[ \frac{1 - \beta_1 \sin 3\theta}{1 - \beta_1} \right]^2$  and

$R_2(\theta) = \left[ \frac{1 - \beta_2 \sin 3\theta}{1 - \beta_2} \right]^2$  denote triaxial compressive strength and triaxial tensile strength, respectively.

The MMC criterion comprises 11 nonlinear parameters, where  $E_{50}^{ref}$ ,  $E_{oed}^{ref}$ , and  $E_{ur}^{ref}$  significantly affect the numerical outcomes. Relying on experience in the same field is necessary to determine appropriate values when selecting parameters. Specific methods for obtaining the values of each parameter are listed in Table 2.

**Table 2.** Methods for taking values of MMC criterion parameters

Parameters	Clarification	Reference point
$E_{50}^{ref}$	Reference cut-line modulus determined by triaxial consolidated drainage shear test	$E_s$
$E_{oed}^{ref}$	Tangent modulus at reference stress determined by standard consolidation tests	$E_{50}^{ref}$
$E_{ur}^{ref}$	Unloading modulus determined by triaxial consolidated drainage loading and unloading tests	$3 * E_{50}^{ref}$

$m$	Modulus stress level correlation power index	0.5/1
$c$	Effective soil cohesion	Reference to MC criterion
$\varphi$	Effective angle of internal friction of soil	Reference to MC criterion
$\psi$	Soil shear angle	$\varphi - 30^\circ$
$R_f$	Destruction ratio	0.9
$p^{ref}$	Reference stress	100Kpa
$KNC$	Lateral pressure coefficient under normal consolidation	$1 - \sin \varphi$
$n$	Porosity	Experimental measurement
$\alpha$	Cap shape factor	Reference to $KNC$
$\beta$	Cap hardening factor	Reference to $E_{oed}^{ref}$

Given the high mechanical strength of strongly, moderately, and slightly weathered granite, the MC criterion is employed in the numerical analysis, while the MMC criterion is employed for the other strata. The major parameter values are listed in Table 3.

**Table 3.** MMC criterion parameters

Geological layer	Secant modulus $E_{50}^{ref}/MPa$	Tangent modulus $E_{oed}^{ref}/MPa$	Unloading modulus $E_{ur}^{ref}/MPa$	Power exponent $m$
Miscellaneous fill	4.56	6.85	45.7	1.0
Sand filling	2.36	3.54	23.6	1.0
Sludge	5.50	8.26	55.1	1.0
Gravelly sand	4.19	6.28	41.9	0.5
Completely weathered	10.0	15.0	1.0	0.5

The numerical model for excavating a shield tunnel includes all the layers present in the shield tunnel section of Shenzhen Bay Bridge. These layers include piles and bearing platforms, the grouting layer within the shield tunnel section, and the shield shell and tube sheet. Implanted beam units are employed to model pile structures, because they accurately represent the mechanical properties of the piles. Combined with the effect range of shield excavation, this study selected 27 piles for four ramp bridges, including 18 existing piles with a diameter of 1.8 m and 9 reinforced piles with a diameter of 1.2 m. The bearing platform, shield shell, and pipe sheet are simulated using plate units. The ring width of the pipe sheet is designed to be 1.8 m, and the thickness of the pipe sheet is 0.65 m. The simulation of the grouting step in shield tunnels can be achieved by configuring the grid properties in the numerical model. The thickness of the grouting layer is 0.29 m, and grouting pressure is stabilized at 0.6 MPa. The details of each structural unit can be found in Table 4.

The displacement boundaries of the model are established by automatic constraints. For example, the X-displacement is constrained in the X-direction, and the Y-displacement is fixed in the Y-direction. A fixed constraint is present at the bottom, while no constraint exists at the top. The bridge pile foundations are cylindrical; hence, rotation constraints should be added to the pile foundations to prevent them from rotating during modeling. The model considers the loads on the pile foundation and the deadweight loads of seawater. Boring thrust and internal and external grouting pressures should be adjusted appropriately during the construction of shield tunnels. The

aforementioned types of loads are then applied to the appropriate grid as necessary.

**Table 4.** Parameters of each structural unit in the model

Structure Type	Compression Modulus $E_s/GPa$	Poisson's ratio $\mu$	Unit weight $\gamma/kN \cdot m^{-3}$	Model category
Pile	30	0.2	25	Implantable beam
Cushion cap	30	0.2	25	Board unit
Grouting layer	32.5	0.2	20	Grid Properties
Shield shell	200	0.3	76.5	Board unit
Segment	36	0.2	20	Board unit

**3.4 Shield tunnel construction**

The shield method is employed in the construction of the tunnels under Shenzhen Bay Bridge. This method involves approximately 70 construction stages, including earth excavation, tube splicing, and grouting. The weight of the bridge on the pile foundation is considered the pile load, while the pressure of seawater is regarded as the seawater load. First, the computational model is balanced for initial soil pressures and then reset for displacement after balancing. Then, the loads acting on the pile and those caused by seawater are applied, and the computational model is re-equilibrated to analyze stress. Subsequently, the overall displacement is reset to zero to ensure the accuracy of subsequent calculations. Finally, tunneling depth is 1.8 m in accordance with the shield tunneling construction principle, with a corresponding tunneling thrust of 0.6 MPa that is released during the next stage of construction. This procedure is repeated until the shield tunnel passes through the bridge piles. The effect of the seepage field is considered during the excavation and lining of the tunnel. The specific construction phases are provided in Table 5.

**Table 5.** Shield tunnel construction

construction stage	Simulate the construction process
1	Initial geo-stress balance (displacement reset)
2	Activate pile and shoreline side pressure load (displacement reset)
3	Steady state seepage
4-70	Simulate the on-site construction process, with a pipe segment ring width of 1.8m as the benchmark, and advance at a distance of 1.8m each time (steady-state seepage)

**4. Result Analysis and Discussion**

Shield tunnels can significantly affect the stability of the pile foundations of a bridge when they pass through preexisting structures. The excessive deformation of bridge piles jeopardizes the safety of existing buildings, particularly when they are improperly constructed. The effects of shield tunnel construction on the deformation of existing bridge piles and ground settlement behavior were highlighted in the current study. The finite element software, Midas GTSNX, was employed to simulate the side penetration of a large-diameter shield tunnel through the pile foundation of an existing bridge.

**4.1 Surrounding ground settlement**

The excavation of the soil layer results in the redistribution of stresses in the surrounding strata, affecting the settlement

of adjacent soil and exerts an influence on the pile foundations of an existing bridge during shield excavation. Moreover, laminar settlement occurs in excavated soil due to the continuous compression of the rigid shield tunnel structure by the surrounding soil (Fig. 4 and Fig. 5).

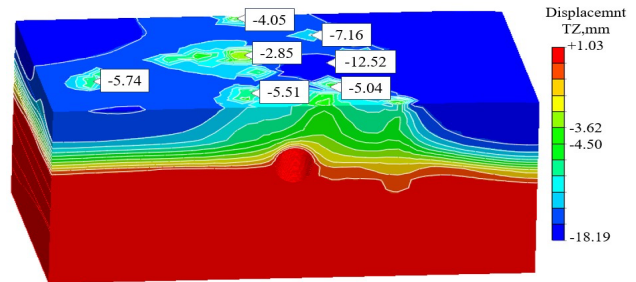


**Fig. 4.** Ground Settlement Clouds from Excavation to 30th Ring

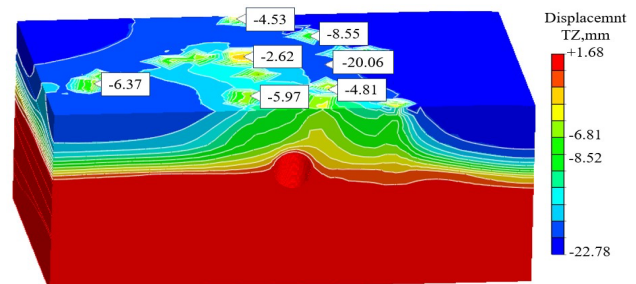


**Fig. 5.** Cloud map of ground settlement after completion of excavation

As shown in Fig. 4, the maximum displacement of the soil above the tunnel is 12.52 mm at the 30th ring of the shield tunnel. As the depth of the stratum increases, the displacement value gradually decreases. The pile settlements for Ramp Bridges B and D, adjacent to the completed tunnel, are 5.04 mm and 5.51 mm, respectively. Meanwhile, the bearing settlements of the ramp bridges at A and C, adjacent to the unconstructed tunnel, are 2.85 mm and 7.16 mm, respectively. The soil in front of the shield tunnel construction experiences settlement due to stress release at the surface of the tunnel excavation, generating active earth pressures on the shield advancement surface. Therefore, adjusting the shield construction in a timely manner is crucial to balance the pressure generated by the soil's thrust displacement. As shown in Fig. 5, the surrounding soil settles further, and the soil above the tunnel settles to 20.06 mm, which is an increase of 60%, when the tunnel crosses Shenzhen Bay Cross-Harbor Bridge. Relatively, the displacement of the bridge abutment changes very little. The settlements of the bearings of Ramps A, B, C, and D adjacent to the tunnel are 2.62, 4.81, 5.97, and 8.55 mm, respectively.

Sections A, B, and C in Fig. 2 are selected to assess the variations in surface settlement during the construction of a shield tunnel, as illustrated in Fig. 6.

As shown in Fig. 6, the surface settlement curves in Sections A, B, and C are affected when a shield tunnel passes through the pile foundations of a bridge. Changes in seawater pressure and soil layers increase soil settlement above the tunnel on the coastal side. Therefore, enhancing the monitoring of the coastal side of the tunnel during the construction period is necessary to ensure construction safety.

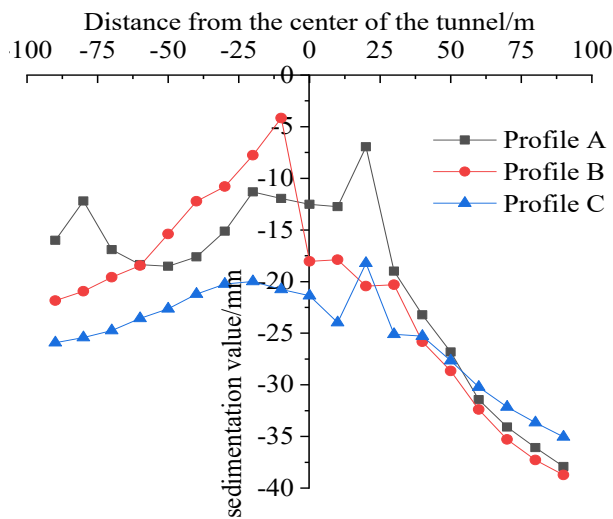


Fig. 6. Vertical displacement variations of profiles A, B and C

**4.2 Analysis of deformation of adjacent pile foundations**

The stress and displacement fields of the surrounding soil constantly change, leading to disturbances and deformations in nearby bridge pile foundations during shield tunnel construction. The state imposes stringent standards for controlling deformation of pile foundations during project construction. The criteria for controlling deformation in this particular project are as follows. Bridge pile settlement should not exceed 10 mm during construction, and horizontal deformation should not exceed 5 mm. Monitoring the horizontal and vertical deformations of nearby pile foundations is important during construction. The deformation of the bridge pile foundations for each ramp (A, B, C, and D) should be observed after shield tunnel construction is completed, as shown in Fig. 7–10.

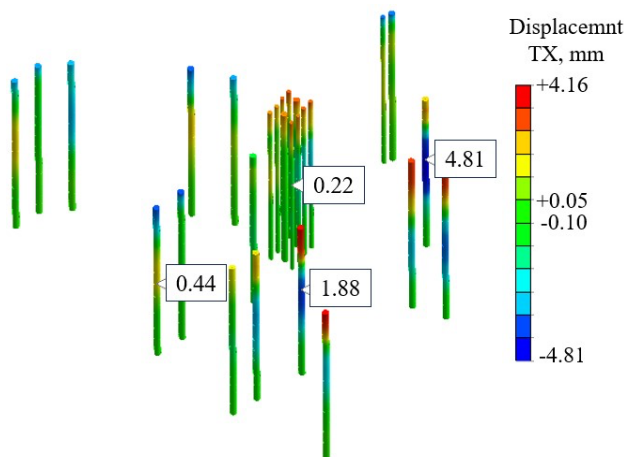


Fig. 7. X-direction deformation cloud map of bridge piles

As shown in Figs. 7 and 8, after completing shield tunnel excavation, the pile foundations of Inclined bridges A, B, C, and D experience greater deformation in the horizontal X-direction compared with in the Y-direction. In addition, the pile foundations on both sides of the top of the shield tunnel exhibit the highest level of deformation. The maximum horizontal displacements for each foundation pile of the ramp bridge in the X-direction are as follows: 0.22, 1.88, 4.81, and 0.44 mm. The results indicate that the horizontal deformation caused by engineering construction is smaller than the maximum allowable limit of 5 mm. The maximum settlement of the bridge pile foundations is 9.77 mm, as

shown in Fig. 9. The pile foundations of Wang Hai Road Bridge consist of end-bearing piles, which are driven deeply into the slightly weathered granite layer. The pile interacts with the surrounding soil, and changes in soil parameters affect the deformation of the pile. This deformation is more pronounced in soft soil layers than in normal soil layers. As shown in Fig. 10, the pile bending moments at the locations on both sides of the shield tunnel excavation face are the largest, while the largest bending moment occurs at the pile foundation of Bridge Ramp C, with a value of 2200 kN·m. The bending moment value decreases with higher compression modulus values for the soil layer due to the varying parameters of the soil layer.

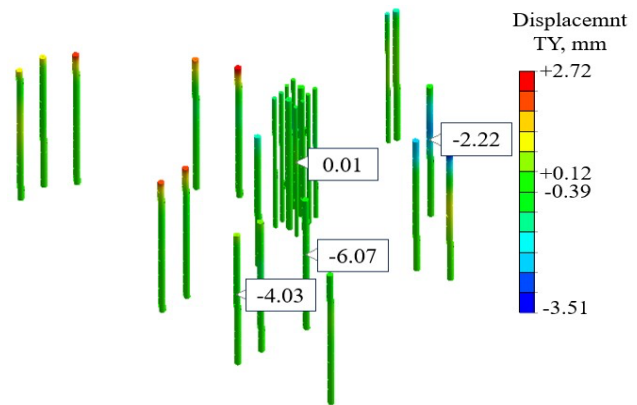


Fig. 8. Y-direction deformation cloud map of bridge piles

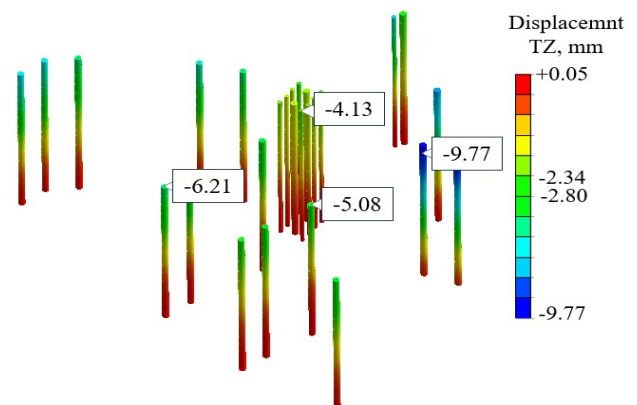


Fig. 9. Z-direction deformation cloud map of bridge piles

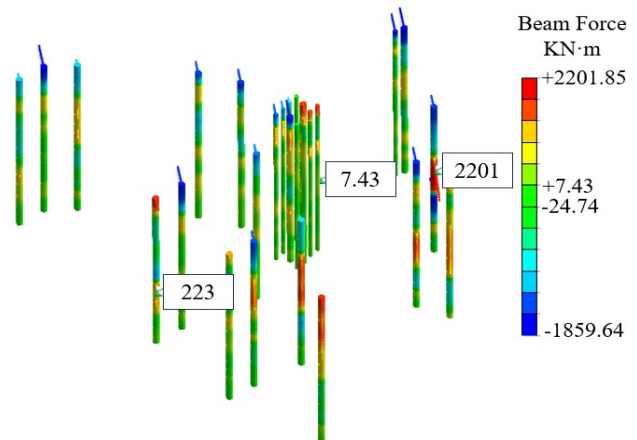


Fig. 10. Bridge pile bending moment -direction deformation cloud map of bridge piles

In addition, Monitoring points A1, B1, C1, and D1 are arranged at the bridge pile foundations closest to the tunnel. These points are used to record the horizontal deformation

pattern of the pile foundations throughout the entire construction process, as shown in Fig. 11.

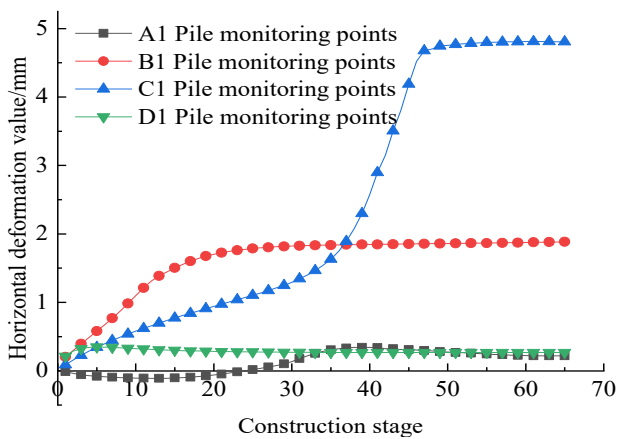


Fig. 11. Horizontal deformation patterns of the pile foundations of bridges at various ramps during different construction stages

In Fig. 11, the shield tunnel passes through bridge pile Monitoring points D1, B1, A1, and C1 in the sequence. The bridge pile foundations of Ramp C are the most affected by shield tunnel construction, followed by the bridge pile foundations of Ramp B. The pile foundations of Ramps A and D are less affected. Overall, the horizontal deformation of bridge pile foundation gradually increases as soil body is excavated before the shield tunnel passes through the foundation. The maximum horizontal deformation of the pile foundation occurs when the tunnel passes through it, and the deformation of the pile foundation remains relatively stable after the tunnel has passed through.

### 4.3 Tunnel construction control measures

During construction, implementing appropriate measures is essential to control ground movement and the deformation of the pile foundation to ensure safety. Considering the large diameter of the shield tunnel at Wanghai Road, the complexity of the regional stratum, and the proximity of the pile foundations to Shenzhen Bay Bridge, implementing the following control measures is necessary during tunnel construction. The specific measures are as follows.

(1) Changing the tool during shield tunneling should be avoided to ensure stable pressure on the palm face.

(2) The experimental section is established prior to construction, and the excavation parameters should be sufficiently adaptable to accommodate any ground deformation or fluctuations in the water table encountered during construction.

(3) The amount of slag must be regulated during excavation to ensure that the digging rate matches the output of slag.

(4) The rate of excavation should be controlled during construction, with the initial excavation occurring at a rate of 1–2 r/d.

(5) Synchronized and secondary grouting must be performed in a timely and sufficient manner during the construction of the shield machine crossing. The use of synchronous grouting is recommended to achieve mobility by using less compressible slurry, while controlling the fill rate within the range of 1.1–1.5, and conducting quality inspections promptly.

(6) A comprehensive real-time monitoring system should be implemented to adjust construction parameters promptly.

## 5. Conclusions

A numerical computational model based on the MMC criterion was proposed to analyze the effect of shield tunnel construction on the stability of existing bridge pile foundations. The deformation evolution law of bridge pile foundations during the entire tunnel construction process was analyzed in the context of an actual project. The following conclusions could be drawn.

(1) An elastic-plastic constitutive model based on the MMC criterion can more effectively describe the surface settlement pattern caused by shield tunnel construction.

(2) The degree of regional ground subsidence caused by shield excavation is determined by two key factors: the distribution of strata and distance from the tunnel. Settlement is greater in areas with complex stratigraphy, and it decreases as distance from the tunnel increases. The coastal area above the tunnel is affected by seawater and experiences significant ground subsidence.

(3) The degree of deformation of bridge pile foundations is influenced by the stage of tunnel construction. The magnitude of bending moment and the deformation of pile foundations decrease as spatial distance from the tunnel increases. The effect on bridge piles decreases as distance from the shield tunnel increases.

(4) During the early stage of shield tunnel construction, pile foundations are in a state of stress equilibrium and are minimally affected by tunnel excavation. During the middle stage of shield tunnel construction, the unloading of soil excavation causes deformations in pile foundations. Pile foundations exhibit the greatest deformation and bending moment on either side of the tunnel. During the late stage of shield tunnel construction, the foundations of bridge piles and the tunnel are restored to a state of stress balance. The settlement and horizontal deformation of pile foundations during tunnel construction comply with engineering specifications.

The entire process of shield tunnel construction was analyzed on the basis of the rapid transformation project of Wanghai Road in Shenzhen. This analysis focused on the deformation of the pile foundations of adjacent bridges and utilized the MMC criterion, which closely aligned with actual engineering conditions. Future shield tunnel construction projects of a similar nature can benefit from the results. However, field monitoring data for pile deformation have not been collected. Field monitoring data and numerical analysis results should be further analyzed in the future, and model parameters should be optimized. The deformation pattern of pile foundations during the close proximity passage of a shield tunnel beneath an existing bridge can be better understood with higher precision.

## Acknowledgements

This work was supported by the National Natural Science Foundation of China (52174069) and the National Key Technologies Research & Development Program (2018YFC0808402).

This is an Open Access article distributed under the terms of the Creative Commons Attribution License.



## References

- [1] Q. Qian and X. Rong, "Current situation, problems and relevant suggestions on safety risk management of underground works in China," *J. Rock Mech. Eng.*, no. 04, pp. 649-655, Apr. 2008.
- [2] W. Guo, K. Hong, P. Gao, F. Li, and X. Zhao, "Status Quo and Prospects of Tunnel Intelligent Construction in China," *Tunn. Constr.*, vol. 43, no. 04, pp. 549-562, Apr. 2023.
- [3] T. Li, "Disturbance Modeling Analysis of Shield Tunnel under High-Speed Railway Bridge Section Considering Stratum Deformation Law," *J. Guangdong Commun Polytech.*, vol. 22, no. 03, pp. 10-14, Aug. 2023.
- [4] L. Wang, F. Zhu, J. Li, and W. Sun, "A data-driven approach for modeling and predicting the thrust force of a tunnel boring machine," *J. Zhejiang Univ.-Sci. A.*, vol. 24, no. 9, pp. 801-816, Aug. 2023.
- [5] C. Yan, *et al.*, "A novel evaluation index of TBM rock-breaking efficiency based on newly added surfaces theory," *Rock. Soil Mech.*, vol. 44, no. 04, pp. 1153-1164, Apr. 2023.
- [6] X. Qu, Y. Wang, Y. Gong, Y. Xia, and S. Yu, "Influence Analysis of Shield Tunneling Parameters on the Deformation of Existing Stations," *Technol. Highw. Transp.*, vol. 38, no. 04, pp. 143-149, Aug. 2022.
- [7] Y. Li, K. Huang, and Y. Sun, "Effect of shield parameters on formation loss rate and surface subsidence in composite strata," *J. Transp Sci. Eng.*, vol. 38, no. 01, pp. 70-78, Mar. 2022.
- [8] G. Wei, D. Zhu, D. Zhao, Z. Wang, and B. Guo, "Research on the soil deformation of overlapped shield tunneling based on unified solution," *J. Zhejiang Univ. Technol.*, vol. 51, no. 05, pp. 489-496, Oct. 2023.
- [9] Y. Rui, J. Yuan, W. Fan, and B. Liu, "Numerical analysis of ground deformation control during the construction of a two-lane tunnel," *Highw.*, vol. 68, no. 06, pp. 455-462, Jun. 2023.
- [10] W. Gao, S. Wang, S. Cui, Y. Wang, S. Ge, and X. Zhong, "Research on Construction Safety of Shield Tunnel Based on DBN," *J. Hebei Univ. Eng (Nat. Sci. Ed.)*, vol. 40, no. 01, pp. 75-80, Mar. 2023.
- [11] G. Yang, H. Li, Z. Yuan, and H. Xiao, "Calculation and Application of Additional Stress on Enclosure Structure of Shield Receiving Work Shaft," *J. Hunan Univ. Nat. Sci.*, vol. 50, no. 09, pp. 152-164, Sept. 2023.
- [12] H. Lu, D. Yuan, F. Wang, and M. Wang, "Study on safe control of metro shield underpassing high-speed railway in weak stratum," *China Civ. Eng. J.*, vol. 48, no. S1, pp. 256-260, Jun. 2015.
- [13] D. Lu, C. Ding, Q. Lin, and X. Du, "Experimental study on three-dimensional effects of shield tunnel excavation on adjacent pile," *J. Disaster Prev. Mitig. Eng.*, vol. 42, no. 04, pp. 732-741, Aug. 2015.
- [14] S. Huang, "A kind of super large diameter shield tunnel through the existing In-situ Protection Construction Technology for Buildings," *China Sci. Technol inf.*, no. 08, pp. 97-102, Apr. 2023.
- [15] T. Wang, "Study on interaction of shield tunnel side crossing existing bridge pile foundation," *J. Saf. Sci. Technol.*, vol. 19, no. S1, pp. 144-149, Aug. 2023.
- [16] Z. Zhou, J. Zhang, H. Ding, and F. Li, "Settlement prediction model of shield tunnel undercrossing existing tunnel based on GA Bi LSTM," *J. Rock Mech. Eng.*, vol. 42, no. 01, pp. 224-234, Jan. 2023.
- [17] G. Wang, Y. Liu, W. Li, W. Rong, and J. Sun, "Study on the influence of construction parameters on the pile group foundation of the shield tunnel passing through buildings at a close angle," *Constr Technol.*, vol. 51, no. 18, pp. 85-89, Sept. 2022.
- [18] C. Zhang, T. Yu, D. Li, Q. Chen, and F. Xue, "Study on the influence of grouting pressure fluctuation on adjacent pile foundations during shield tunneling," *Chin. J. Undergr. Space. Eng.*, vol. 18, no. 02, pp. 596-602, Apr. 2022.
- [19] X. Zhou, J. Yang, and T. Liu, "Analysis of the influence of shield tunneling on the pile foundation of a short distance side crossing bridge," *Chin. J. Undergr. Space. Eng.*, vol. 18, no. 02, pp. 586-595, Apr. 2022.
- [20] K. Huang, *et al.*, "Impact of shield tunnel excavation based on seepage stress coupling on adjacent bridge pile foundations," *J. Cent. South Univ. (Sci. Technol.)*, vol. 52, no. 03, pp. 983-993, Mar. 2021.
- [21] L. Yang, *et al.*, "Centrifuge model test study on construction of super large diameter shield tunnel under railway," *Mod. Tunn. Technol.*, vol. 58, no. 04, pp. 170-177, Aug. 2021.
- [22] Y. Gao, X. Zhang, J. Li, and Y. Zhou, "Study on the surface deformation of the river under the shield tunnel in silty clay layer," *Min Res. Dev.*, vol. 42, no. 06, pp. 79-84, Jun. 2022.
- [23] M. A. Soomro, C. W. W. Ng, K. Liu, and N. A. Memon, "Pile responses to side-by-side twin tunnelling in stiff clay: Effects of different tunnel depths relative to pile," *Comput. Geotech.*, vol. 84, pp. 101-116, Apr. 2017.
- [24] G. T. K. Lee and C. W. W. Ng, "Effects of advancing open face tunneling on an existing loaded pile," *J. Geotech. Geoenviron. Eng.*, vol. 131, no. 2, pp. 193-201, Feb. 2005.
- [25] P. Simic-Silva, B. Martinez-Bacas, R. Galindo-Aires, and D. Simic, "3D simulation for tunnelling effects on existing piles," *Comput. Geotech.*, vol. 124, pp. 103625, Aug. 2020.
- [26] L. Repetto, A. Tuninetti, V. Guglielmetti, and G. Russo, "Shield tunnelling in sensitive areas: A new design procedure for optimization of the construction-phase management," in *Saf. Undergr. Space-Proc. ITA-AITES 2006 world Tunn Congr. 32th ITA Gen Assem*, Seoul, Korea, 2006, pp. 270
- [27] N. Allahverdi, B. Bakhshi, M. Partovi, and V. Nasri, "3D-nonlinear finite element analysis of staged shield-driven tunnel excavation with a focus on response of segmental tunnel lining," *Geomech. Tunn.*, vol. 16, no. 01, pp. 60-67, Jan. 2023.
- [28] H. Lee, J. Oh, Y. J. Shin, and J. Won, "Laboratory Investigation on Excavation Performance of Foam-conditioned Weathered Granite Soil for EPB Shield Tunnelling," *KSCE J. Civ. Eng.*, to be published. Accessed: Aug. 14, 2023. doi: 10.1007/s12205-023-2163-9. [Online]. Available: <https://link.springer.com/article/10.1007/s12205-023-2163-9>
- [29] Z. Zizka, B. Schoesser, and M. Thewes, "Investigations on transient support pressure transfer at the tunnel face during slurry shield drive part I: Case A – Tool cutting depth exceeds shallow slurry penetration depth," *Tunn. Undergr. Space Technol.*, vol. 118, Dec. 2021, Art. no. 104168.
- [30] Z. Zizka, B. Schoesser, M. Thewes, and T. Schanz, "Slurry Shield Tunneling: New Methodology for Simplified Prediction of Increased Pore Pressures Resulting from Slurry Infiltration at the Tunnel Face Under Cyclic Excavation Processes," *Int. J. Civ. Eng.*, vol. 17, no. 01, pp. 113-130, Jan. 2019.
- [31] A. A. Lavasan, C. Zhao, T. Barciaga, A. Schaufler, H. Steeb, and T. Schanz, "Numerical investigation of tunneling in saturated soil: the role of construction and operation periods," *Acta Geotech.*, vol. 13, no. 03, pp. 671-691, Jun. 2018.
- [32] L. C. E. F. Filho, M. E. Hartwig, and C. A. Moreira, "EPB excavation in transitional mixed face: Line 5-Lilac (São Paulo Metro, Brazil)," *Bull. Eng. Geol. Environ.*, vol. 81, no. 05, May. 2022.
- [33] N. Bilgin and S. Acun, "The effect of rock weathering and transition zones on the performance of an EPB-TBM in complex geology near Istanbul, Turkey," *Bull. Eng. Geol. Environ.*, vol. 80, no. 04, pp. 3041-3052, Apr. 2021.
- [34] G. H. Erharter, R. Goliash, and T. Marcher, "On the Effect of Shield Friction in Hard Rock TBM Excavation," *Rock Mech. Rock Eng.*, vol. 56, no. 04, pp. 3077-3092, Jan. 2023.
- [35] D. Bach, W. Holzer, W. Leitner, and N. Radončić, "The use of TBM process data as a normative basis of the contractual advance classification for TBM advances in hard rock," *Geomech. Tunn.*, vol. 11, no. 05, pp. 505-518, Oct. 2018.